

# Physical and technological interpretation of mechanical properties for single and multi-layer films with properties of dry lubricants

A. O. MATEESCU<sup>a,b</sup>, G. MATEESCU<sup>a</sup>, V. JINGA<sup>b\*</sup>, D. CRISTEA<sup>b</sup>, C. SAMOILĂ<sup>b</sup>, D. URSUȚIU<sup>a</sup>, D. MUNTEANU<sup>b</sup>  
<sup>a</sup>*AEG Progresiv S.R.L., 6 Nucsoara Street, B. 42 / E / 70, 060524 Bucharest, Romania*  
<sup>b</sup>*Transilvania University of Brasov, 29 Eroilor Blvd., 500036, Brasov, Romania*

The starting point of this research was a project for the Romanian Space Agency regarding improvement of lubrication properties of the materials used in extreme conditions (e.g. in outer space). As a further idea, this approach is also healthy for Earth's environment, by replacing oil lubricants and so, pollution caused by all these will decrease. Another place for applications can be cutting tools from the industrial domain – where temperatures of both cutting tool and part are decreased during the machining process by using cooling fluids, which are expensive, can be toxic and produce a significant waste stream (not healthy). The proposed solution for all of these problems are multilayer films, special coatings deposited in such a way, under aspect of used materials and deposition conditions, that they become dry lubricants. For this reason, the research team did some experimental depositions using simple and compound materials (Ti, TiB<sub>2</sub>, WC, WS<sub>2</sub>) through Standard or Reactive DC and RF Magnetron Sputtering Method, in presence or not of N<sub>2</sub> as a reactive gas. Probes were then tested and analyzed by the CSM Table Top Platform equipment. All results were taken into consideration for improving the deposition methodology and for obtaining good multilayer films that have characteristics of dry lubricants.

(Received April 9, 2015; accepted June 24, 2015)

**Keywords:** Dry lubricant coatings, Multilayer coatings, Wear resistance

## 1. Introduction

Scratch test technique is an old and proper method for characterizing mechanical properties of materials. Although its widespread use and apparent simplicity, a fundamental understanding of the physical mechanism underlying this type of test has not been fully developed [1].

A scratch test is done by drawing a diamond indenter across a coated surface under an increasing load (continuous or stepwise) until at a specific load  $L_c$  – critical load, a well defined failure event occurs. If coating detachment represents the failure, then the critical load can be used for a qualitative measure regarding coating – substrate adhesion. An entire range of failure modes can occur and only some are adhesion dependent. Other failure modes dependent on plastic deformations and fractures within the coating may be as useful in determining the coating's quality particularities for tribological applications [2].

The reliability of the scratch test method was investigated during an European project, FASTE, where the conclusion was that the variation concerning the stylus type shape, due to incorrect radius or damage, is the main source of uncertainty in this test method [3].

Another research project was set up (REMAST), having as objectives the development and certification of a “real world” reference material regarding the verification of proper scratch test instruments functioning by detecting

deviations in stylus tip shape and errors concerning load, displacement calibrations or other instrument malfunctions [4]. As the main conclusion, a considerable improvement of the scratch stylus quality can be achieved by strict control of all manufacturing steps. Also, a diagnostic tool is useful, providing a means of sensitive monitoring for machine and stylus performance over extended periods of time.

In another study, P. Lu et al revealed that when coating delamination occurs, high intensity acoustic emission (AE) signals can be clearly detected. Tangential force increases gradually with the normal force and fluctuates significantly when the critical load for coating delamination is reached. Authors developed a three-dimensional (3D) finite element (FE) model with a cohesive-zone interface for simulating the scratch process and by comparing the delamination critical load obtained experimentally, interface characteristic length, the maximum strength and fracture energy can be determined. The results indicated that it's feasible to use FE simulations combined with effective scratch tests in order to better evaluate the behavior at the coating interface [5].

The mechanical behavior of multilayer coatings (tungsten – carbon based) was studied by E. Harry et al, and good adhesion between the hardest and thickest multilayer coating and the substrate was observed. Also, it's stated that such coatings having many layers exhibit resistance to erosion [6].

In this paper, the authors will thoroughly describe the manner in which the depositions were made, the tests that were done (not only scratch tests, but also friction coefficient determinations, elastic modulus and hardness testing) and will comment on the obtained results from the tests, concluding with the influence of deposition parameters regarding the coating's properties.

These contributions describe a new approach in designing tribological coatings based on single and multilayered structures made of Ti/TiB<sub>2</sub>/WC/WS<sub>2</sub>, respectively Ti<sub>x</sub>N<sub>y</sub>/Ti<sub>x</sub>B<sub>y</sub>N<sub>z</sub>/W<sub>x</sub>C<sub>y</sub>N<sub>z</sub>/W<sub>x</sub>S<sub>y</sub>N<sub>z</sub>. Their properties and perspectives for application are taken into account based on author's contributions in several patents [7].

## 2. Experimental procedures

### 2.1. Materials and process parameters

Substrates: stainless steel plates were used and, before each deposition, were ultrasonic and glow discharge cleaned. During the deposition process, the substrates were in a rotation movement (to obtain a homogenized coating), 20 rot/minute. The substrates were heated at 550 °C and the bias voltage was set at 0.5 kV during each deposition.

Deposition method: a multifunctional vacuum thin film deposition system, having four (3 DC and 1 RF – all with maximum power of 600 W) sputtering magnetrons (guns). Ar was used as a bombardment gas and N<sub>2</sub> as a reactive gas. The distance between the substrate and the target was set at approximately 10 – 15 cm. This method allows deposition of multilayer in one working experimental cycle.

In this paper, depositions of three samples and their properties will be discussed, one single layer type, the other two being multilayer coatings:

Sample no. 1 – one layer composed in an unique way from 4 materials deposited simultaneously:

1 x (Ti + TiB<sub>2</sub> + WC + WS<sub>2</sub>);

Sample no. 2 – multilayer having 30 layers, organized in 6 repetitive packages with 5 layers per package, each layer having a variable composition out of 4 materials:

6 x {5 x [(Ti<sub>x</sub>N<sub>y</sub> + Ti<sub>x</sub>B<sub>y</sub>N<sub>z</sub> + W<sub>x</sub>C<sub>y</sub>N<sub>z</sub> + W<sub>x</sub>S<sub>y</sub>N<sub>z</sub>)<sub>i</sub>, i = 1 – 5]};

Sample no. 3 – multilayer having 20 layers, organized in 5 repetitive packages with 4 layers per package, each layer having a variable composition out of one material:

5 x (Ti<sub>x</sub>N<sub>y</sub>/ Ti<sub>x</sub>B<sub>y</sub>N<sub>z</sub>/W<sub>x</sub>C<sub>y</sub>N<sub>z</sub>/W<sub>x</sub>S<sub>y</sub>N<sub>z</sub>).

The working process parameters for the magnetron sputtering deposition method used to obtain the above mentioned samples are presented in Table 1.

Table 1. Working process parameters for deposition of samples no. 1, 2 and 3

Sample No.	Materials	Working gases		Power injected in the gun's plasma [%P <sub>max</sub> ]	Deposition time [min]	Working pressure [mbar]
	Deposited layers	Ar [sccm]	N <sub>2</sub> [sccm]			
1	1 x (Ti + TiB <sub>2</sub> + WC + WS <sub>2</sub> )	150	0	1 x (10 + 20 + 20 + 16)	55	3.4 x 10 <sup>-3</sup>
2	6 x {5 x [(Ti <sub>x</sub> N <sub>y</sub> + Ti <sub>x</sub> B <sub>y</sub> N <sub>z</sub> + W <sub>x</sub> C <sub>y</sub> N <sub>z</sub> + W <sub>x</sub> S <sub>y</sub> N <sub>z</sub> ) <sub>i</sub> , where i = 1 – 5]}	110	80	6 x [(45 + 5 + 5 + 5) / (30 + 30 + 10 + 10) / (20 + 45 + 20 + 23.3) / (10 + 30 + 30 + 25) / (5 + 5 + 45 + 30)]	180 (6 min. per layer)	2.4 x 10 <sup>-3</sup>
3	5 x (Ti <sub>x</sub> N <sub>y</sub> / Ti <sub>x</sub> B <sub>y</sub> N <sub>z</sub> / W <sub>x</sub> C <sub>y</sub> N <sub>z</sub> / W <sub>x</sub> S <sub>y</sub> N <sub>z</sub> )	110	80	5 x (15 + 30 + 30 + 20)	100 (5 min. per layer)	2.4 x 10 <sup>-3</sup>

### 2.2. Characterization methods

The mechanical and tribological properties of the coated samples described above were investigated by the following methods: Scratch Test Method, Hardness Test Method and Pin-on-disk Tribometer.

Mechanical and tribological parameters: the analyses were done using CSM Table Top Platform which includes the standard Nanoindentation head (NHT2) and the standard Micro scratch tester head (MST) into a small and simple-to-use instrument [8, 9].

Scratching method: the micro scratch tester head (MST) has a Rockwell type indenter. The Micro Scratch

Tester (0 – 30 N) is suited for analyzing thin hard or soft coatings. It contains a full software package for data acquisition and analyses of mechanical properties [10, 11]. The Nanoindentation Tester (0.05 – 500 mN) provides low loads with depth measurement in the nanometric scale. The system can be used to characterize organic, inorganic, hard and soft materials.

Tests were done with the Rockwell indenter (100 Cr6 material) having a 100 μm tip radius. The linear scratch was progressive, having the begin load 0.03 N for all samples, the end load variable – 15 N for sample no. 1, 10 N for sample no. 2, 25 N for sample no. 3 and the loading rate constant for all samples at 4.99 N/min. AE Sensitivity

was 9 and the scratch length was 3 mm for each test, only the speed varied from 1 mm/min for sample no. 1 to 1.5 mm/min for sample no. 2 till 0.6 mm/min for sample no. 3.

For each sample, three scratch tests were done using the same settings for each measurement.

After carrying out the tests, the critical loads could be established:  $L_{c1}$  – the load when the first cracks are noticed,  $L_{c2}$  – the load necessary for the first delamination (the first section of film removed from the substrate),  $L_{c3}$  – load necessary for removal of more than 50% of film from the scratch track.

Nanoindentation technique: NHT2 – the standard Nanoindentation head, mounted on a stainless steel cantilever is used in order to obtain good statistics.

Nanoindentation measurements were performed with a diamond tip Berkovich indenter, penetration depth being constant (no greater than 10% of coating estimated thickness, in order to minimize the effect of the substrate on the results) [12]. It is specified that the estimated thickness of coatings was taken into consideration because thickness measurements done using CSM Table Top Platform have no good precision in case of coating's thicknesses lower than 800 nm.

Between 6 and 8 measurements were performed on each sample, with the following protocol: loading/unloading speeds of 100 nm/min with a pause of 2 s between the loading and unloading stages.

The penetration depth was constant during tests done on each probe: for sample no. 1 the penetration depth was  $73 \text{ nm} \pm 1\%$ , for sample no. 2 it was  $100 \text{ nm} \pm 1\%$  and for sample no. 3,  $75 \text{ nm} \pm 4\%$ .

All samples (1 to 3) were indented using the Auto Indent Mode option, allowing to set up the number of the lines, columns and the space between them.

Tribometer method: a sphere, a pin or a flat section is loaded onto the test sample with a precisely known force. The probe is mounted on a stiff lever, designed as a frictionless force transducer. The friction coefficient is determined during the test by measuring deflection of the elastic arm. Wear coefficients for the pin and disk materials are calculated from the volume of material lost during the test. This simple method facilitates the study of friction and wear behavior of almost every solid material combination with or without lubricant.

On each sample, 2 or 3 tests were performed using 6 mm 100 Cr 6 steel balls as counterparts, in rotation mode, normal load being 1 N. Atmospheric conditions were constant during all tests,  $24 \text{ }^\circ\text{C}$  temperature, 32% humidity, acquisition rate being 200 Hz. The variable parameters were the Radius [mm] (8/6 mm for sample no. 1, 6/10/12 mm for sample no. 2, 12/10 mm for sample no. 3), the Linear Speed [cm/s] (6 cm/s for sample no. 1 and 20 cm/s for samples no. 2 and 3) and the Stop Condition [m] meaning the length of the wear track (1/3 m for sample no. 1, 3 m for sample no. 2 and 6/4 m for sample no. 3). No lubricating solutions were used for these measurements.

### 3. Results and discussions

#### 3.1. Adherence: scratch tests

For sample no. 1,  $L_{c1}$  values varied from 0.37 N to 0.55 N, mean value being calculated at  $0.466 \text{ N} \pm 20\%$  measurement error.  $L_{c2}$  variation started at 0.55 N up to 0.84 N, mean value being  $0.683 \pm 23\%$  and  $L_{c3}$  from 6.67 N up to 7.52 N, with a mean value of  $6.96 \text{ N} \pm 8\%$  error.

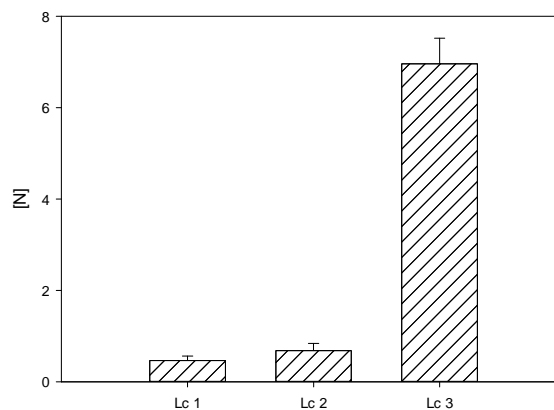


Fig. 1. Scratch test's results, sample no. 1

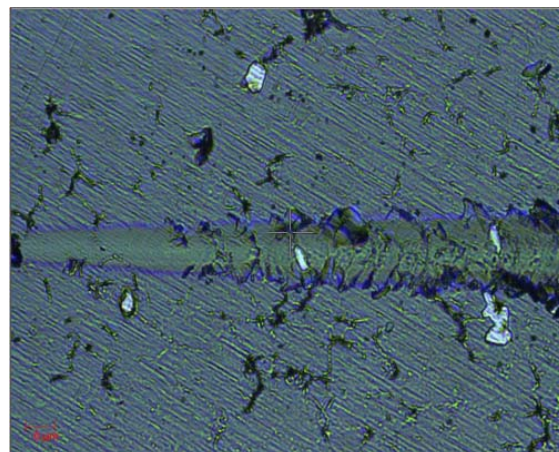


Fig. 2. Critical loads for sample no. 1 ( $L_{c1}$ ,  $L_{c2}$ )

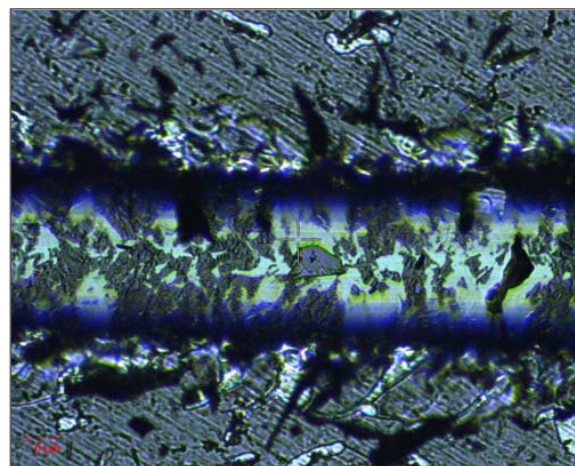


Fig. 3. Critical loads for sample no. 1 ( $L_{c3}$ )



For sample no. 2 scratch tests weren't relevant, because the points where first crack and delamination occur couldn't be established with precision (Fig. 4 and 5 state this fact).  $Lc_3$  varied from 5.73 N up to 6.79 N, mean value being calculated at  $6.396 \text{ N} \pm 10\%$ .

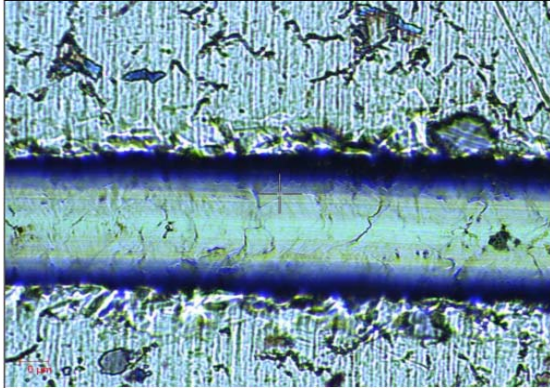


Fig. 4. Scratch test results, sample no. 2 ( $Lc_3$ )

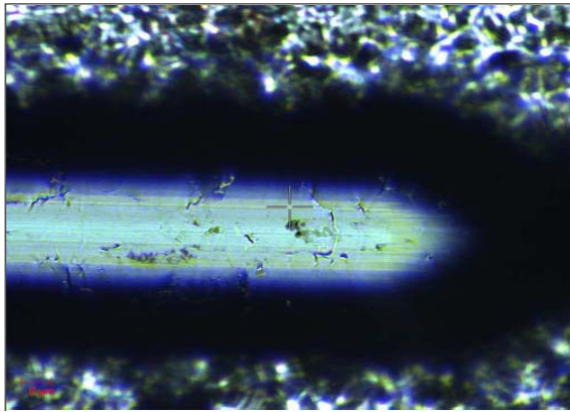


Fig. 5. Scratch test finalization, sample no. 2

For sample no. 3 scratch tests weren't totally conclusive regarding first crack appearance – critical load  $Lc_1$  (see Fig. 7 and 8) couldn't be established.

$Lc_2$  values varied from 0.39 N to 0.54 N, mean value being  $0.486 \pm 20\%$  determined measurement error and  $Lc_3$  had a variation starting at 5.23 N up to 6.67 N, calculated mean value being  $6.073 \pm 14\%$ .

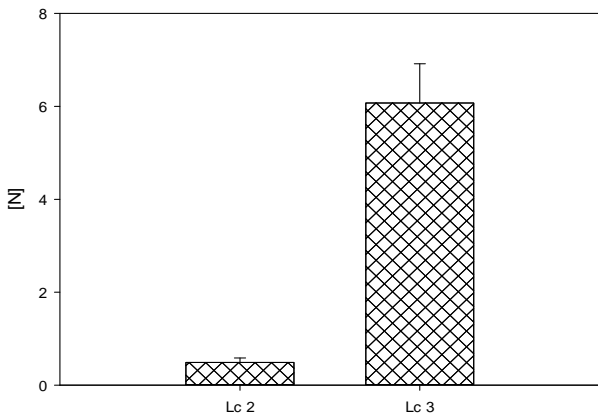


Fig. 6. Scratch test's results, sample no. 3

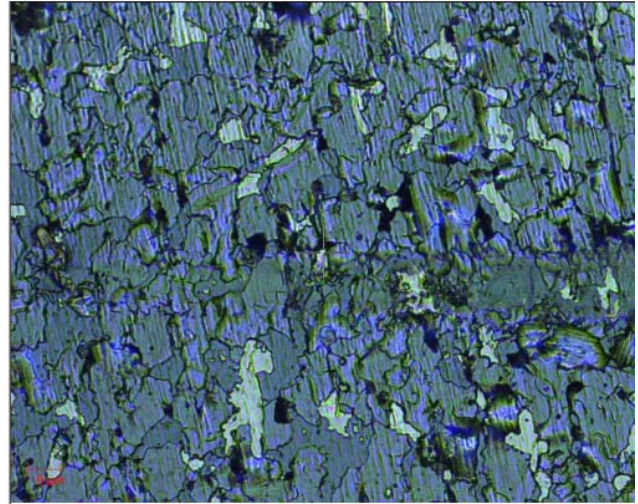


Fig. 7. Critical loads for sample no. 3 ( $Lc_2$ )

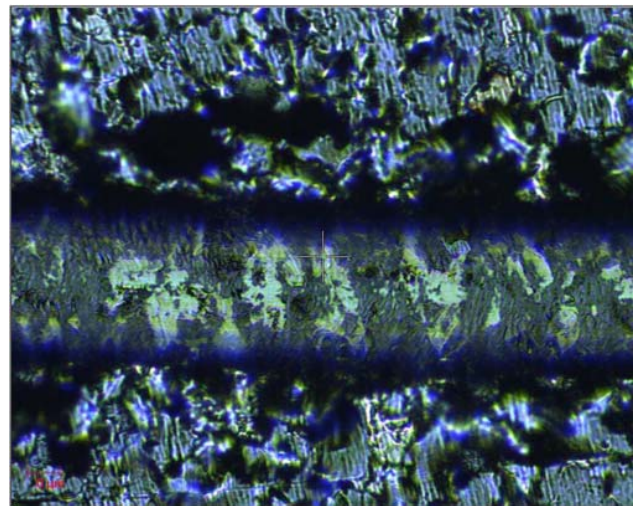


Fig. 8. Critical loads for sample no. 3 ( $Lc_3$ )

### 3.2. Hardness indentation and elastic modulus

Eight indentations were performed on sample no. 1. Hardness values varied from 11464 MPa to 12808 MPa, mean value being  $12040.75 \text{ MPa} \pm 6.5\%$  error.

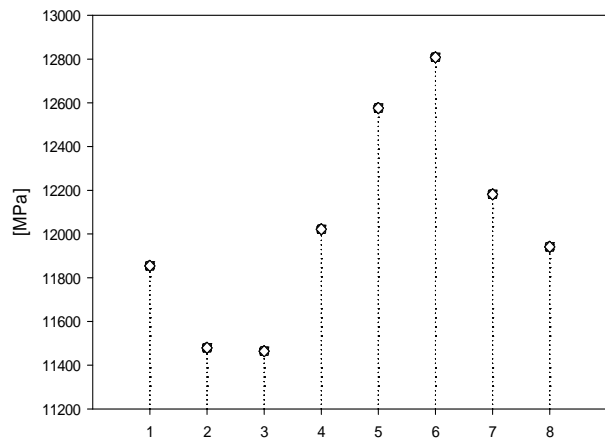


Fig. 9. Hardness test's results, sample no.1

Elastic modulus had values starting at 169.02 GPa up to 212.48 GPa, its mean value being calculated at  $195.9175 \pm 14\%$ .

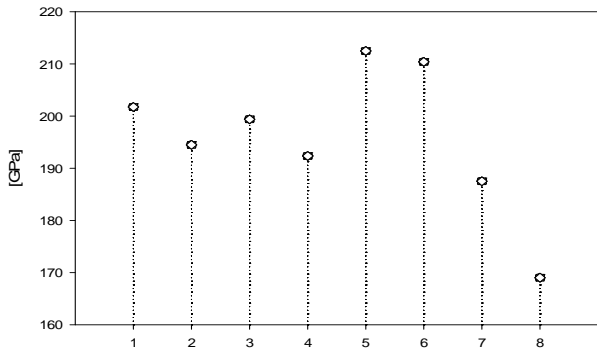


Fig. 10. Elastic modulus results, sample no. 1

For sample no. 2, only six indentations were done. Hardness varied from 3394.8 MPa to 3610.5 MPa, having a mean value of  $3516.117 \text{ MPa} \pm 3.5\%$ .

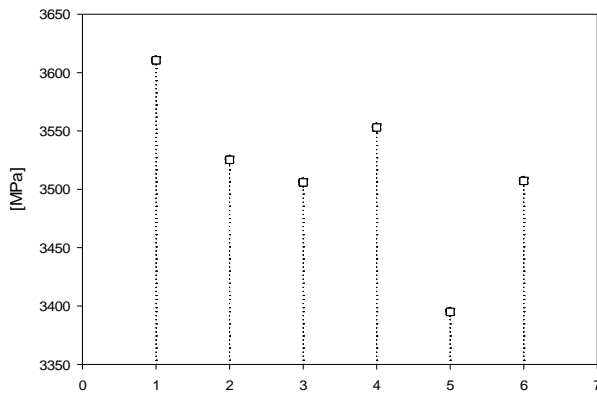


Fig. 11. Hardness test's results, sample no. 2

Values for elastic modulus started at 204.98 GPa and ended at 244.69 GPa, mean value being  $221.7133 \text{ GPa} \pm 10\%$  error.

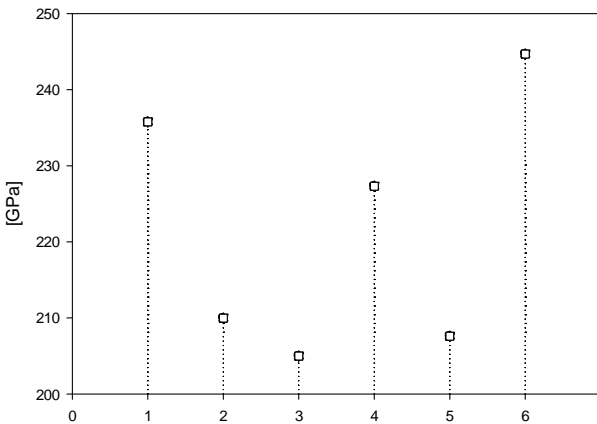


Fig. 12. Elastic modulus results, sample no. 2

Six indentations were performed for sample no. 3 also. Hardness variation was between 4489.4 MPa and 5789.4 MPa, mean value being  $5011.483 \text{ MPa} \pm 15\%$ .

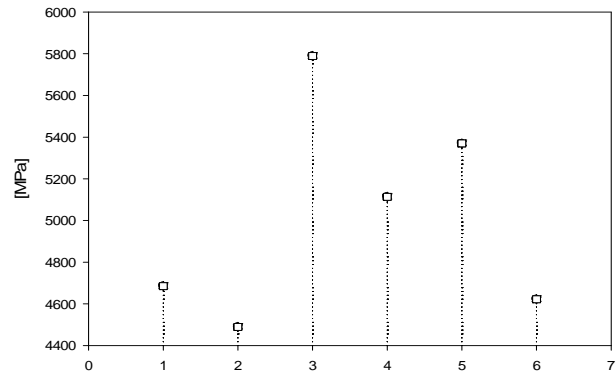


Fig. 13. Hardness test's results, sample no. 3

Elastic modulus values varied from 164.89 GPa up to 211.9 GPa, mean value being calculated at  $195.655 \text{ GPa} \pm 16\%$  error.

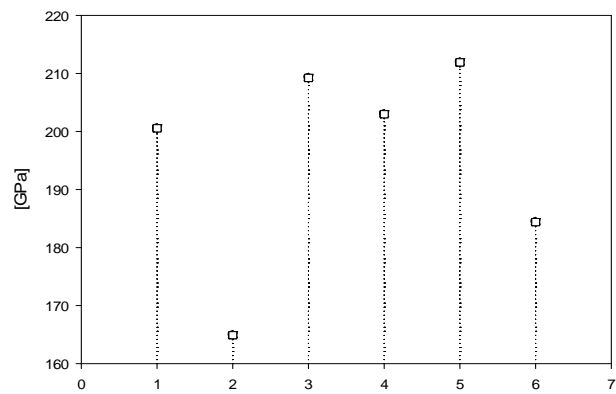


Fig. 14. Elastic modulus results, sample no. 3

### 3.3. Friction coefficients

On sample no. 1 only two wear tests were performed.  $\mu_{\min}$  coefficient didn't vary at all, having values between 0.146 and 0.149, its mean value being  $0.1475 \pm 1\%$  error.  $\mu_{\max}$  coefficient varied between 0.214 and 0.285, having a mean value of  $0.2495 \pm 14\%$ .  $\mu_{\text{average}}$  coefficient started at 0.177 up to 0.231, its mean value being calculated at  $0.204 \pm 13\%$ .

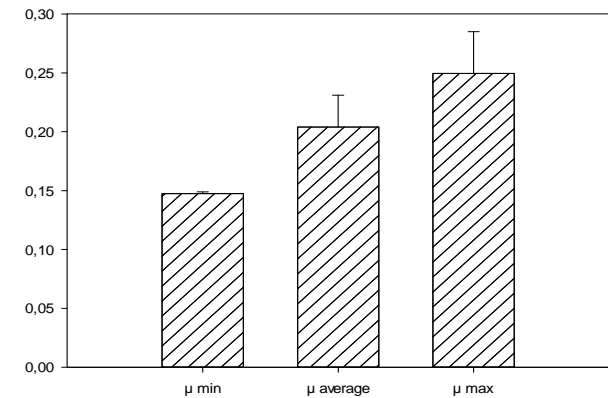


Fig. 15. Friction coefficients, sample no. 1



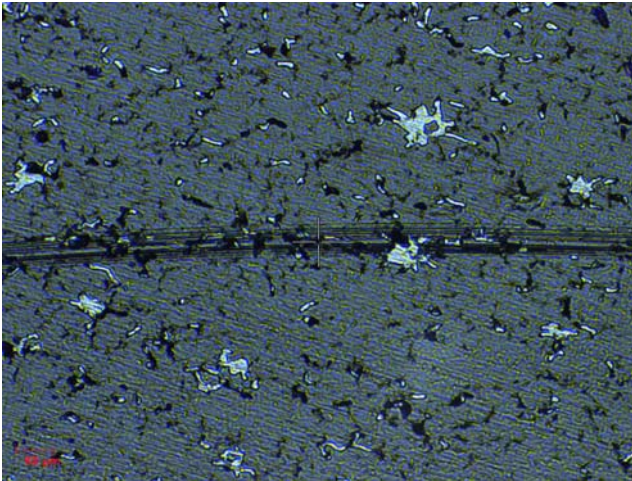


Fig. 16. Wear track for sample no. 1 (length 1 m)

Two wear tests were done for sample no. 2 also.  $\mu_{\min}$  coefficient values varied from 0.195 to 0.291, its mean value being  $0.243 \pm 20\%$ .  $\mu_{\max}$  coefficient varied between 1.012 and 1.086, mean value being  $1.049 \pm 2\%$  error.  $\mu_{\text{average}}$  coefficient had values starting at 0.642 up to 0.67, its mean value being calculated at  $0.656 \pm 3.5\%$ .

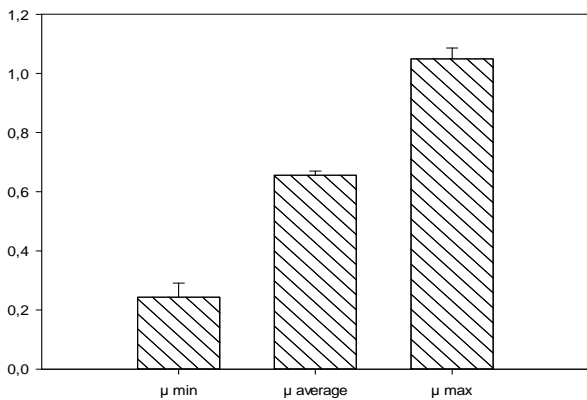


Fig. 17. Friction coefficients, sample no. 2

For sample no. 2 friction coefficient's values don't vary so much, but  $\mu_{\text{average}}$  has rather a large value (a significant inconvenient for dry lubrication purposes).

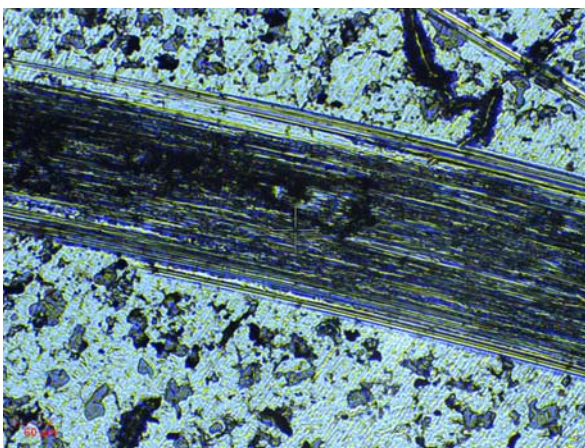


Fig. 18. Wear track for sample no. 2 (length 6 m)

On sample no. 3 three wear tests were performed.  $\mu_{\min}$  coefficient had values between 0.037 and 0.238, with a mean value of  $0.15 \pm 75\%$  (error generated by the lowest value registered).  $\mu_{\max}$  coefficient varied from 0.866 to 1.244, mean value being calculated at  $1.0276 \pm 21\%$ .  $\mu_{\text{average}}$  coefficient variation started from 0.587 up to 0.661, having a mean value of  $0.6173 \pm 7\%$  error.

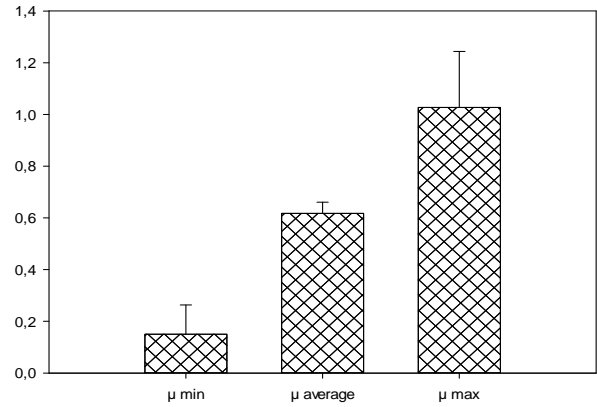


Fig. 19. Friction coefficients, sample no. 3

For sample no. 3,  $\mu_{\text{average}}$  coefficient has a rather large value (around 0.6) being an inconvenient for dry lubricants.

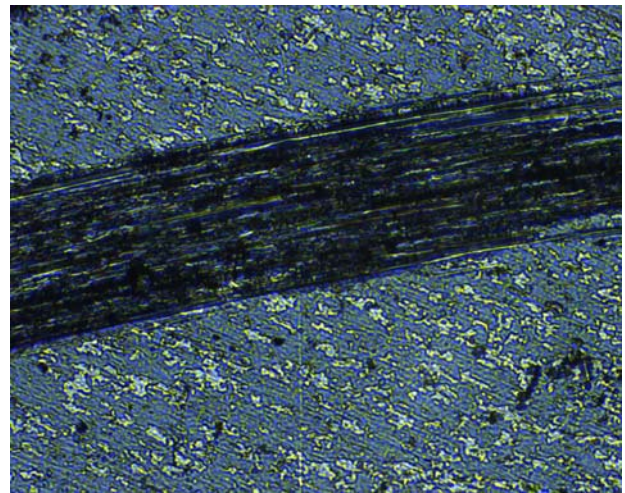


Fig. 20. Wear track for sample no. 3 (length 3 m)

### 3.4. Comparative discussions

As illustrated in Fig. 21 to 23 there is a big difference between values obtained for  $L_{c1}/L_{c2}$  and  $L_{c3}$  for all samples, due to lubricant properties of the coatings. Practically,  $L_{c3}$  value is more than 20 times higher than  $L_{c1}/L_{c2}$  values. Also, values of critical loads ( $L_{c1}$ ,  $L_{c2}$ ,  $L_{c3}$ ) are lower comparing to the values reported for TiN [12]. The highest values of  $L_{c1}$ ,  $L_{c2}$ ,  $L_{c3}$  were obtained for sample no. 1 (single-layer) when deposition process took place without nitrogen at the lowest total working gas flow (150 scfm). As one can see from Table 1, the reactive gas ( $N_2$ ) has not participated at increasing the total pressure (sample no. 2 and 3) because it is incorporated in the deposited film.

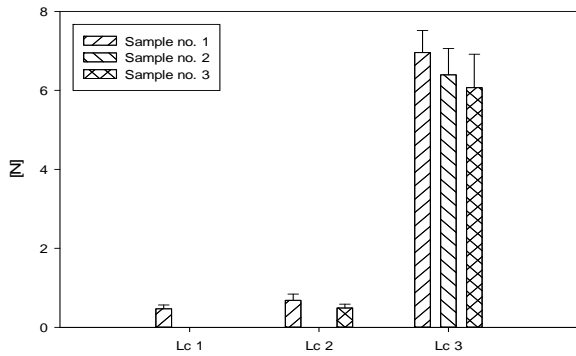


Fig. 21. Scratch test's comparative results

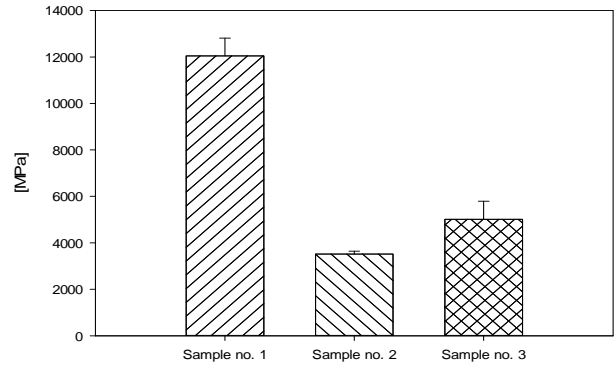


Fig. 24. Hardness test's comparative results

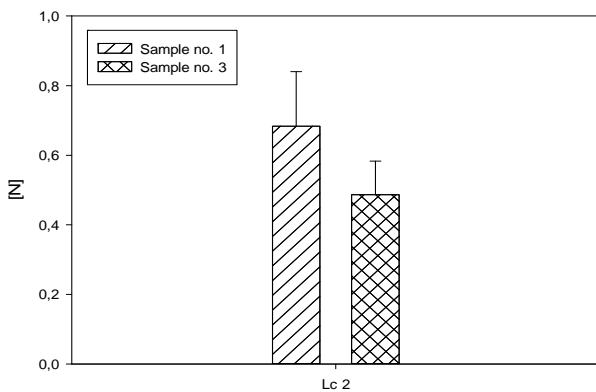


Fig. 22. Lc<sub>2</sub> scratch test's comparative results

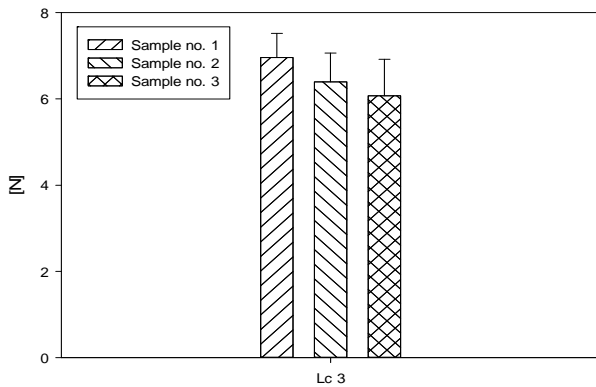


Fig. 23. Lc<sub>3</sub> scratch test's comparative results

Hardness test's comparative results for all the samples revealed highest hardness obtained for sample no. 1, containing a unique layer of 3 compound materials (WC, TiB<sub>2</sub> and WS<sub>2</sub>) and 1 metallic material (Ti), without N<sub>2</sub>.

Values of elastic modulus for all samples were very close one to another, as shown in Fig. 25.

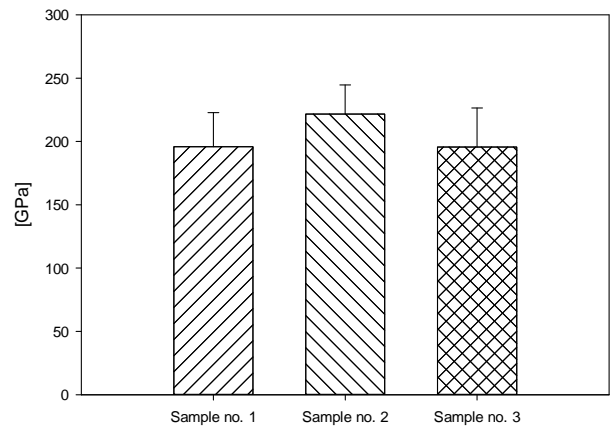


Fig. 25. Elastic modulus comparative results

Obtained values of hardness and elastic modulus for all samples are a little higher than the values reported in the literature [13-18] for most part of the component materials deposited as individual unique thin films (TiN, WC and TiB<sub>2</sub>); they have similar values with those obtained for WS<sub>2</sub> and are lower than the values reported for Ti, as it is presented in Table 2.

Maximal values of friction coefficient were obtained after removal of coating material from substrate (because of low coating's thickness) and in this case, the maximal friction coefficient ( $\mu_{max}$ ) corresponds to friction between steel ball and substrate; for this reason only  $\mu_{min}$  coefficient is analyzed and its values are lower than the ones reported in literature and presented in Table 2.

Table 2. Reference values for hardness, elastic modulus and friction coefficients

Measured Parameters	Individual constituent materials					Sample no.		
	WS <sub>2</sub>	Ti	TiN	WC	TiB <sub>2</sub>	1	2	3
Hardness [GPa]	15.3 [13] ; 5.8 [14]	2.4 - 3.4 [15]	31 [16]	14.6 - 23.6 [17]	22 - 2 [18]	12	3.5	5
Elastic modulus [GPa]	166 [13]	100 - 125 [15]	300 - 400 [16]	259 - 350 [17]	570 - 360 [18]	195	222	196
Friction coefficient ( $\mu_{min}$ )	0.62 - 0.78 [13]	-	0.65 - 0.70 [19]	0.15 - 0.35 [17]	0.75 - 0.80 [18]	0.145	0.255	0.145

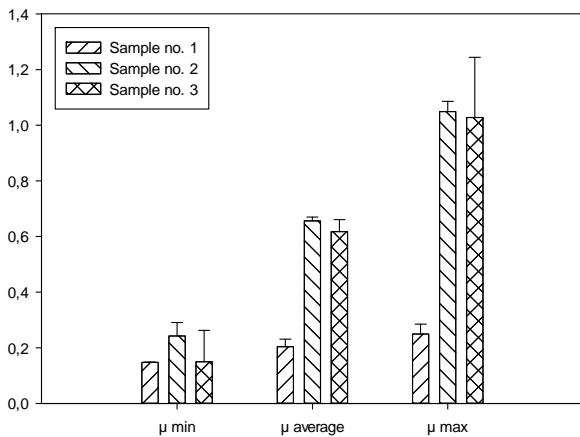


Fig. 26. Friction coefficients comparative results

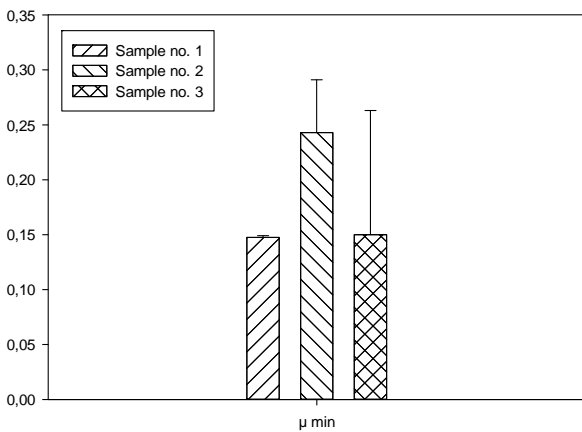


Fig. 27.  $\mu_{min}$  coefficient's comparative results

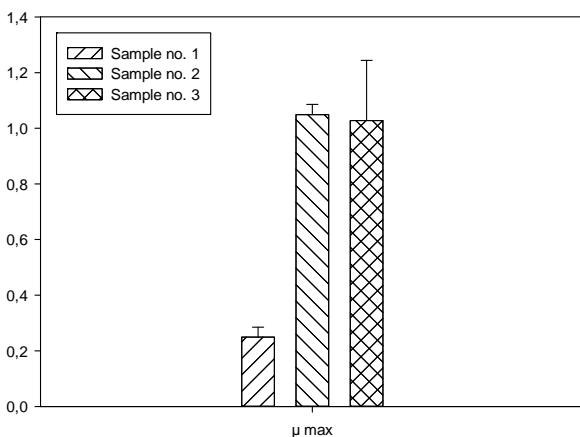


Fig. 28.  $\mu_{max}$  coefficient's comparative results

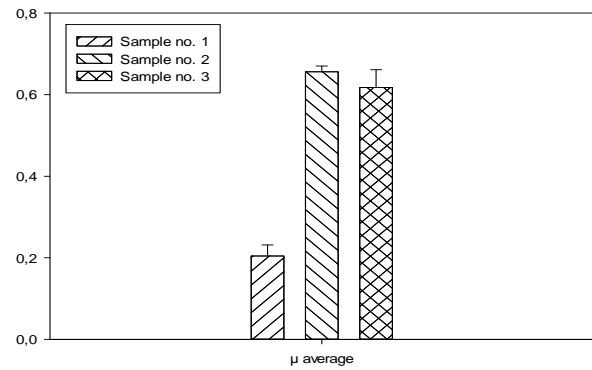


Fig. 29.  $\mu_{average}$  coefficient's comparative results

#### 4. Conclusions

Friction coefficient obtained for all samples prove that lubricant properties are present for all coating structures and process parameters that were used (see Table 1). Sample no. 1 having a single layer of 3 compound materials (WC, TiB<sub>2</sub> and WS<sub>2</sub>) and 1 metallic material (Ti) deposited without nitrogen as a reactive gas, has the best mechanical characteristics (hardness and elastic modulus) as also the best lubricant properties (the lowest value for friction coefficient). The decreasing of the mechanical characteristics, by reduction of the hardness and increasing of the friction coefficient especially for sample no. 2, comparative with the sample no. 1 is due to the reactive gas N<sub>2</sub> that at high deposition temperature (550 °C) introduces stress in the deposition films that reduce the mechanical properties of the films, especially their adherence to the substrate. Also, it is considered that insignificant modification of the reactive deposition process parameters (when N<sub>2</sub> was used) for a short period, (because this process is not as stable as a non-reactive deposition process) could produce significant modification of the mechanical characteristics of the deposited films. This means that the deposition parameters of the reactive deposition processes must be carefully observed and stabilized for the entire process period.

#### Acknowledgements

“This paper is supported by the Sectoral Operational Programme Human Resources Development (SOP HRD), financed from the European Social Fund and by the Romanian Government under the project number POSDRU/159/1.5/S/134378”. We hereby acknowledge the structural funds project PRO-DD (POS-CCE, O.2.2.1., ID 123, SMIS 2637, ctr. No 11/2009) for providing the infrastructure used in this work and the project. This work was supported by a grant of the Romanian National Authority for Scientific Research, Program for research - Space Technology and Advanced Research - STAR, project number 68/2013.



## References

- [1] <http://cee.mit.edu/onbalance/2011/december>
- [2] S. J. Bull, *Tribology International* **30**(7), 491 (1997).
- [3] J. Meneve, et al., K.L. Mittal (Ed.) VSP International Science Publishers, Zeist, The Netherlands, *Adhesion Measurement of Films and Coatings*, **2**, 79 (2001).
- [4] European Commission – Standards, Measurements and Testing Program, Project ‘A Certified Reference Material for the Scratch Test—REMAST’, contract **SMT4-CT98/2238**, completed 31/12/2001.
- [5] P. Lu, X. Xiao, M. Lukitsch, A. Sachdev, Y. K. Chou, *Thin Solid Films*, **206**(7), 1860 (2011), DOI: 10.1016/j.surfcoat.2011.08.022.
- [6] E. Harry, A. Rouzaud, P. Julliet, Y. Pauleau, *Thin Solid Films*, **342**(1), 207 (1999), DOI: 10.1016/S0040-6090(98)01499-0.
- [7] a) G. Mateescu, A. O. Mateescu, Vacuum coating method of metallic pieces with lubricant thin films, Patent No. **128144/30.06.2013**.  
 b) A. O. Mateescu, G. Mateescu, Coating multilayer material with tribological properties and procedure for its achievement, Patent No. **128094/30.09.2014**.  
 c) G. Mateescu, A. O. Mateescu, Lubricant and wear resistant compound from wolfram disulfide, carbon and metal, Patent No. **1279623/30.12.2014**.  
 d) G. Mateescu, A. O. Mateescu, Dry, Lubricant and Complex Materials with structure of monolayer and gradual or constant composition and methods or procedures for achievement of the gradual and lubricant coatings with these materials, Patent Application No. **A/01074/28.12.2012-OSIM**.  
 e) G. Mateescu, A. O. Mateescu, Materials and methods for achievement of the gradual and complex tribological coatings of the metallic objects that work under friction, Patent Application No. **A/01075/28.12.2012-OSIM**.
- [8] CSM Instruments, Application Bulletin No. **18** (September 2002), No. 37 (January 2012).
- [9] W.C. Oliver, G. M. Pharr, *J. Mater. Res.*, **19**, (2004).
- [10] C.C. Schmitt, J.R. Elings, M. Serry, *Nanoindenting, Scratching, and Wear Testing with the Atomic Force Microscope*, **AN13**, Rev A1 (2004).
- [11] K. Abdelouahdi, C. Sant, C. Legrand-Buscema, P. Aubert, J. Perrière, G. Renou, Ph. Houdy, *Surface & Coatings Technology* **200**, 6469–6473 (2006).
- [12] The certification of critical coating failure loads: a reference material for scratch testing according to ENV **1071-3**; European Commission; Report EUR 20986 REFERENCE MATERIALS (1994).
- [13] Zhu Li-na, Wang Cheng-biao, Wang Hai-duo, Xu Bin-shi, Zhuanh Da-ming, Liu Jia-jun, Li Guo-lu, *Vacuum* **85**, 16 (2010) DOI: 10.1016/j.vacuum.2010.03.003.
- [14] Ratoi Monica, V. B. Niste, J. Zekonyte, *RSC Advances*, **4** (41):21238-21245 (2014), DOI: 10.1039/C4RA01795A.
- [15] R. C. Chang, F. Y. Chen, C. T. Chuang, Y.C. Tung, *Journal of Nanoscience and Nanomaterials.*, **10**, 4562 (2010).
- [16] P. H. Mayrhofer, H. Clements, *Int. Journal of Materials Research and Advanced Techniques* (2005).
- [17] T. Tavsanoglu, C. Begum, M. Alkan, O. Yucel (2013), DOI:10.1007/2013.
- [18] R. G. Murno, *Journal of Research-National Institute of Standard Technology*, Vol. **105**, No.5
- [19] Priev Surface Engineering- Functional coatings [www.priev.com/en/coatings/functional-pvd](http://www.priev.com/en/coatings/functional-pvd).

\*Corresponding author: jingavlad@yahoo.com